

## Short time structural relaxation processes in liquids: Comparison of experimental and computer simulation glass transitions on picosecond time scales

C. A. Angell and L. M. Torell

Citation: *J. Chem. Phys.* **78**, 937 (1983); doi: 10.1063/1.444798

View online: <http://dx.doi.org/10.1063/1.444798>

View Table of Contents: <http://jcp.aip.org/resource/1/JCPSA6/v78/i2>

Published by the American Institute of Physics.

---

### Additional information on J. Chem. Phys.

Journal Homepage: <http://jcp.aip.org/>

Journal Information: [http://jcp.aip.org/about/about\\_the\\_journal](http://jcp.aip.org/about/about_the_journal)

Top downloads: [http://jcp.aip.org/features/most\\_downloaded](http://jcp.aip.org/features/most_downloaded)

Information for Authors: <http://jcp.aip.org/authors>

## ADVERTISEMENT

**physicstoday**

Comment on any  
*Physics Today* article.

The advertisement shows a red arrow pointing from the text 'Comment on any Physics Today article.' to a comment box on a sample article page. The sample article is titled 'Measured energy in Japan' by David von Seggern. The comment box contains a comment by Edgar McCarroll dated 14 July 2012 19:59, discussing the energy release of a 100-megaton explosion and the relationship between seismic energy and nuclear energy.

# Short time structural relaxation processes in liquids: Comparison of experimental and computer simulation glass transitions on picosecond time scales

C. A. Angell

*Department of Chemistry, Purdue University, West Lafayette, Indiana 47907*

L. M. Torell

*Department of Physics, Chalmers University of Technology, Fack, S-402 20 Gothenburg, Sweden*

(Received 28 July 1982; accepted 6 October 1982)

Recent Brillouin scattering studies of relaxation in the simple ion system  $\text{Ca}^{++}\text{-K}^{+}/\text{NO}_3^{-}$  (two particles of argon structure and a small anion) provide the experimental basis for a direct comparison of glass transformation phenomenology in computer simulated LJ argon "glass," with that in laboratory substances studied on the same time scale. Most of the attenuated glass transition characteristics observed for LJ argon are found in the ionic system, and the same relation of the dispersion midpoint to the so-called "ideal" glass transition temperature is observed. Analysis of the real and imaginary parts of the complex longitudinal modulus shows that at high temperatures the relaxation function for  $\text{Ca}^{++}\text{-K}^{+}\text{-NO}_3^{-}$ , in strong contrast with that at normal low temperature behavior, closely approaches a simple exponential decay with Arrhenius form for the relaxation time. Furthermore, the high temperature Arrhenius plot extrapolates naturally to the reciprocal quasilattice vibration frequency determined by far infrared absorption studies on the glassy solid. Because of the low activation energy in the high temperature regime the glass "transition" observed with decreasing temperature is smeared out almost beyond recognition. It is argued that this will be a rather general phenomenon for hyperquenched glasses and that for such cases, the fictive temperature concept which associates the glass structure with an internally equilibrated liquid structure (that at  $T_{\text{fictive}}$ ) must collapse. Parallels between LJ argon and  $\text{Ca}^{++}\text{-K}^{+}\text{-NO}_3^{-}$  glasses are discussed.

## INTRODUCTION

The glass transition is usually thought of as a phenomenon associated with very slow molecular rearrangement processes, and high viscosities, of order  $10^{13}$  P.<sup>1</sup> The discovery, and recent exploitation, of metallic glasses formed by very fast ("splat") quenching processes of order  $dT/dt = -10^7$  deg s<sup>-1</sup>,<sup>2,3</sup> and the advent of even faster quench rates in laser melting<sup>4</sup> and computer simulation studies<sup>5-11</sup> has shifted the focus of attention to the process of structural arrest on very short time scales. Because of obvious experimental difficulties, it has not yet been possible in the laboratory to observe under fast cooling the equivalent of the normal heat capacity  $C_p$ , or expansion coefficient  $\alpha$ , anomalies usually used to characterize the glass transition, and thus to form a concept of the nature of the "transition" occurring under such conditions.

Apart from the knowledge gap, lack of this information is detrimental to discussion of the feasibility of successfully bypassing crystallization during cooling. Certain computer simulation studies have indicated<sup>5</sup> that a very rapidly cooled glass can continue to relax and even nucleate crystals at temperatures as low as  $0.1 T_m$ , (below both its anticipated "normal" and also "ideal" glass transition temperatures) because of the high entropy state of the not-quite-"frozen" material. If this is the case, then the chances of bypassing crystallization in every case are clearly much reduced and new data relevant to this question are therefore needed. It has often been asserted that *any* liquid can be vitrified if the cooling rate is made high enough, but such statements are made without adequate consideration of the possible changes in the relaxation-determined character

of the glass transition on very short time scales. It is with the characterization of the "fast" glass transition, and the associated problem of establishing the appropriate description of the liquid relaxation response over very wide temperature and relaxation time scales, that the present paper is concerned.

Recent computer simulation studies of simple Lennard-Jones (LJ) argon during stepwise<sup>6,7</sup> and continuous<sup>6,8</sup> cooling, at very high effective cooling rates  $10^{10}\text{-}10^{12}$  deg s<sup>-1</sup>, have indicated that the glass transition is very "smeared out" in temperature, and relaxation occurs continuously over an interval of temperature amounting to about one half of the temperature at mid-relaxation. This contrasts strongly with the normally observed experimental glass transition in which the state of internal equilibrium characteristic of the liquid is completely lost in an interval of temperature which may be as little as 5% of the "glass transition temperature."

It was tempting at first to associate this contrast in behavior, and also the apparent lack of hysteresis effects which are characteristic of the "normal" glass transition,<sup>9,10</sup> with the simple form of the LJ interatomic potential. Specifically, the lack of hysteresis suggested that a zero order parameter or continuous equilibrium transition between liquid and glass states definable by a single line on the phase diagram as in Ref. 9 might occur in such cases. The alternative possibility<sup>10,11</sup> is that a smeared-out glass transition and consequent difficulty in observing hysteresis effects might be encountered in laboratory glass-forming systems, notwithstanding their more complex potentials, simply by studying them on the same time scale as is characteris-

tic of the simulations.

It is noteworthy, therefore, that experimental measurements on a system of simple spherical or quasi-spherical particles, conducted on the same time scale as the simulations, have recently become available and confirm in all necessary detail the computer simulation observations. We refer to the Brillouin scattering studies by one of us<sup>12</sup> of liquid  $\text{Ca}^{++}\text{-K}^{+}\text{-NO}_3^{-}$  solutions (of  $\text{Ca}^{++}/\text{K}^{+} = 2:3$  mole ratio) in which the first two constituents have the argon electronic structure and the third, a thick triangular anion with rotation volume roughly that of  $\text{Br}^{-}$ , serves to neutralize the positive charge. The long range Coulomb potential provides a fairly flat background potential on which the dynamics are determined primarily by the repulsive interactions<sup>11</sup> as in argon under external pressure. Before introducing, comparing, and analyzing the respective results, however, it is necessary briefly to discuss relaxation processes under different thermodynamic stresses, and consider their respective time scales.

### THERMAL AND MECHANICAL RELAXATION PROCESSES

We first show that the time scale of the Brillouin scattering studies is the same as that of the system response during the typical computer simulation cooling schedule in which "computer glass transitions" have been detected.

Analysis of the dependence of apparent heat capacity of glass-forming liquids on cooling and heating rate shows that the glass transition temperature defined by the onset of the heat capacity rise for the common scan rate of  $10 \text{ deg min}^{-1}$  corresponds to the temperature at which the relaxation time of the supercooled liquid is  $\sim 200 \text{ s}$ .<sup>13,14</sup> The (mid-transformation range) temperature at which the high temperature (liquid) and low temperature (glassy) parts of the enthalpy and volume plots intersect is a little higher and corresponds to a relaxation time of  $\sim 20 \text{ s}$ . The latter construction seems the best way of defining the glass transition in computer simulated glass-forming processes.<sup>10</sup> Now, a scan rate of  $10 \text{ deg min}^{-1}$ , or  $0.2 \text{ deg s}^{-1}$ , which we call  $q_{1ab}$ , is nearly 13 orders of magnitude slower than the equivalent simulation quench (typically<sup>7,11</sup> a sequence of  $10 \text{ deg temperature changes followed by } 10 \text{ ps equilibrations which yields an average quench rate, } q_{sim} \sim 10^{12} \text{ deg s}^{-1}$ ). If the relaxation time  $\tau_{1ab}$  at the ordinary  $T_g$  is  $200 \text{ s}$  and at mid-range is  $20 \text{ s}$  then the relaxation time at the simulation glass transition will be of order  $\tau_{1ab} \times q_{1ab}/q_{sim} = (4-40) \text{ ps}$ . This ranges over the same order of magnitude time scale as that of Brillouin scattering measurements. Indeed for the  $90^\circ$  scattering observations in the  $\text{Ca}^{++}\text{-K}^{+}\text{-NO}_3^{-}$  solution, the most strongly absorbed phonon, i.e., that corresponding to the condition  $\omega_B \tau_L = 1$  where  $\tau_L$  is the relaxation time, has a frequency of  $8.7 \text{ GHz}$ , i.e.,  $\tau_L = 17 \text{ ps}$ .<sup>12</sup>

The glass transition usually recorded in the laboratory, and also that simulated with the computer, results directly from a failure, in the "glass transformation range," to achieve full thermodynamic equilibrium during the continuous cooling, such that below a certain temperature  $T_g$  the system exhibits the thermodynamic

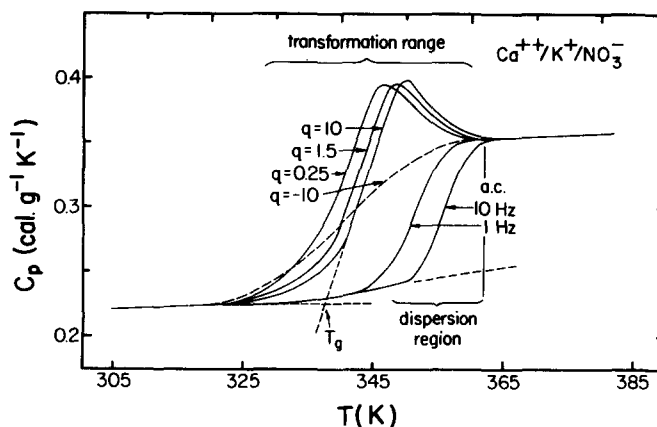


FIG. 1. Heat capacity variations through the glass transition region as determined by normal differential scanning calorimetry at three different heating rates and one cooling rate, compared with expected variation of heat capacity measured by an ac technique at 1 and 10 Hz. For continuous cooling processes, the temperature region affected by the slow structural relaxation is called the "transformation range," while for the case of ac measurements it is called the "dispersion region." [The  $q$  data are for a  $\text{Ca}^{++}\text{-K}^{+}\text{-NO}_3^{-}$  ( $\text{Ca}^{++}/\text{K}^{+} = 2:3$ ), glass studied by C. T. Moynihan, A. J. Eastale, M. A. Debolt, and J. C. Tucker, *J. Am. Ceram. Soc.* **59**, 16 (1976).

properties of a solid. On the other hand, in a fixed frequency experiment, as is approximately the case in Brillouin scattering, a system initially in full thermal equilibrium is subjected to an oscillatory mechanical perturbation (pressure waves, or "phonons," generated by coupling to the light beam), the response to which will be solidlike, liquidlike, or complex depending on the liquid structural relaxation time at the temperature of measurement. By changing the temperature at (approximately) constant frequency, a progressive change-over from a liquidlike (hot) to a solidlike (cold) response can be observed. The change will occur at a temperature which is higher than the normal glass transition by an amount depending on the frequency of the perturbation. The difference between the Brillouin experiment and the calorimetric glass transition phenomenon is that as soon as the pressure wave is "turned off" the substance is again in full thermodynamic equilibrium (assuming  $T > T_g$  as is usually the case). A closer and more obvious relation between the thermal and mechanical relaxation experiments would be obtained if the heat capacity were measured by an ac method<sup>15</sup> using small oscillatory temperature perturbations during slow cooling. Such a measurement would find the heat capacity decreasing to solidlike values at temperatures higher (about  $10^\circ$  higher for a  $10 \text{ Hz}$  experiment), than the normal glass transition temperature. Here also the system would be in full thermodynamic equilibrium if the perturbation were suddenly turned off (provided  $T > T_g$ ). The relation between ac and normal cooling/heating  $C_p$  plots is shown in Fig. 1, using data for the  $\text{Ca}^{++}\text{-K}^{+}\text{-NO}_3^{-}$  system. What is referred to as the glass transformation range in the direct cooling/heating experiment, is usually referred to as the "dispersion region" in the ac type of experiment (to date performed only for dielectric and mechanical stresses).

In the Brillouin experiment which is conducted at about

10 GHz, it is the velocity of sound which is seen to change from liquidlike to solidlike values, and the change is observed at temperatures far above the normal  $T_g$ . The sound velocity for longitudinal phonons,  $v_L$  is related to a compressibilitylike intensive thermodynamic property, the longitudinal compliance  $\beta_{L,s}$ , by the relation

$$\beta_{L,s} = \frac{1}{\rho v_L^2}, \quad (1)$$

where  $\rho$  is the density and the subscript  $S$  indicates that the quantity is an adiabatic property. At high temperatures, above the dispersion region,  $\beta_{L,s}$  becomes identical with more familiar adiabatic compressibility  $\kappa_s$ . In the relaxation region  $v_L$  will show a dispersion and  $\beta_{L,s}$  will be a complex quantity,  $\beta_{L,s}^* = \beta'_{L,s} + i\beta''_{L,s}$ . If  $\beta_{L,s}$  were to be determined from the velocity of 10 Hz rather than 10 GHz sound waves, then its real part  $\beta'_{L,s}$  would be observed to change from liquidlike to solidlike values at a much lower temperature. The changes would then be expected in the same temperature range in which  $C_p$  changes at 10 Hz, since the relaxation time for enthalpy in viscous liquid systems seems to be closely similar to those for structural relaxation near the glass transition.<sup>16</sup>

With this background we can now go ahead and compare laboratory and simulation relaxation data in the short time regime.

## COMPARISON OF LABORATORY AND COMPUTER SIMULATION SHORT TIME RELAXATIONS

The details of the elevated temperature Brillouin doublet measurements and the velocity dispersion and absorption results for the glass-forming system  $\text{Ca}^{++}\text{--K}^+\text{--NO}_3\text{--}(\text{Ca}^{++}/\text{K}^+ = 2/3)$  were given in earlier papers.<sup>12,17</sup> Here we reproduce the longitudinal phonon velocity and absorption data in Fig. 2(a) and the corresponding (frequency-dependent) longitudinal compliance  $\beta_{L,s}$  (real part) in Fig. 2(b). Figure 2(b) also contains a plot of the familiar adiabatic compressibility  $\kappa_s$  (real part), which is obtained by combining longitudinal and transverse<sup>20</sup> sound velocity data using  $\kappa_s = [\rho(v_L^2 - 4/3 v_T^2)]^{-1}$ , see Ref. 21. For contrast we show in Fig. 2(c) the variation of the constant pressure heat capacity with temperature at the normal  $T_g$  for this system<sup>22,23</sup>. The contrast is striking, and shows the smearing out effect associated with the shift of the dispersion region to the short time, high fluidity, region discussed recently in relation to the computer glass transitions.<sup>10,11</sup> The variation of  $\kappa_s$  with  $T$  when measured on a long time scale as for  $C_p$  can be judged from a combination of ultrasonic and static determinations [see  $\kappa_{s,0}$  Fig. 2(b)].

In Fig. 3 the results for  $C_p$  and the volume expansivity  $\alpha$  of the LJ system, with parameters characteristic of argon, taken from recent studies of Clarke<sup>7</sup> and of Fox and Andersen,<sup>8</sup> are shown as a function of temperature, and are compared with the variation of the  $\sim 10$  GHz  $\kappa_s$  for  $\text{Ca}^{++}\text{--K}^+\text{--NO}_3$  taken from Fig. 2(b). (The Fox-Andersen study used both stepwise and continuous cooling at rates up to 100 times slower than the stepwise cooling schedule of Clarke and therefore their results would more appropriately be compared with the upper fre-

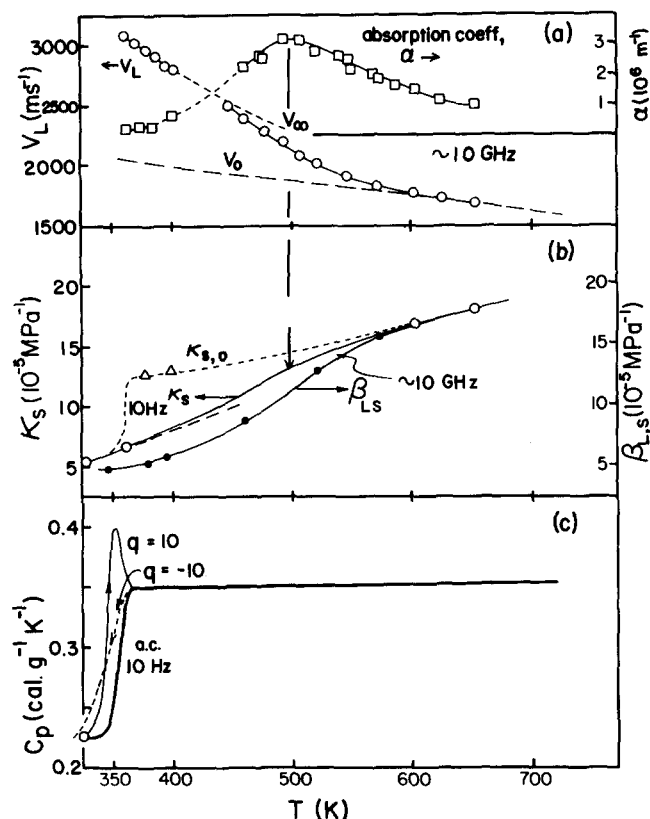


FIG. 2. Dependence of the "sharpness" of the glass transition for  $\text{Ca}^{++}\text{--K}^+\text{--NO}_3$  on the frequency at which the experiment is conducted. Part (a) shows the hypersonic sound velocity  $v_L$  and absorption coefficient  $\alpha$  determined at GHz frequencies while part (b) shows the adiabatic and longitudinal compressibilities  $\kappa_s$  and  $\beta_{L,s}$  at GHz frequencies, and also the low frequency adiabatic compressibility  $\kappa_{s,0}$ . Part (c) shows the known heat capacity variations during constant scan rate, and the projected ac heat capacity at 10 Hz (from Fig. 1).

quency limit of ultrasonic data. There is also a displacement due to the use of a truncated LJ potential in Ref. 8.) The temperature scale for the ionic liquid data in part(c) has been chosen so that, starting from zero, the mid-point in the dispersion [where the absorption maximum in Fig. 2(a) occurs], falls approximately in mid-diagram, as for the LJ data. Figure 3 shows that the hypersonic  $\kappa_s$  dispersion is comparable with the  $C_p$  variation in the hyperquenched LJ glass transition cf. Fig. 2(b). Note the distinction between ac and  $T$ -scan data at low  $T$ , described in the figure caption.

It is reasonable to conclude from Figs. 2 and 3, that the smeared-out glass transition, in which molecular rearrangements can continue down to quite low temperatures even during the fastest quenches, will be the general case for hyperquenched glasses. Network liquids which have large activation energies will provide exceptions but these are few in number. It is important now to characterize the dispersion in this fast relaxation regime for the general case as far as the available data allow, and then to account as broadly as possible for the difference in character of the ultra-fast cooling and normal glass transition phenomena.

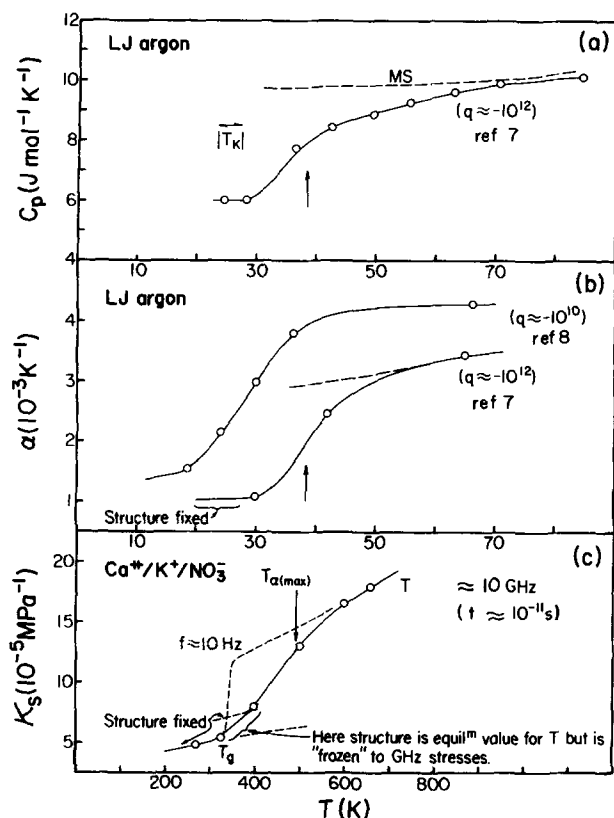


FIG. 3. Heat capacity (a) and expansivity (b) variations through the glass transition for LJ argon from computer simulation methods (Refs. 7 and 8) at quenching rates of  $10^{10}$ – $10^{12}$   $\text{deg s}^{-1}$ , compared with (c) the variation of the adiabatic compressibility  $\kappa_s$  at hypersonic frequencies for  $\text{Ca}^{++}\text{--K}^{+}\text{--NO}_3^{-}$  from Fig. 2(b). To make the comparison more appropriate, we include in the latter diagram (c) the projected variation of the adiabatic compressibility at fixed structure (dashed line), judged by observations of the sound velocities below the normal glass transition temperature (Ref. 20). This is necessary because the adiabatic compressibility below the dispersion region in the case of the hypersonic experiment corresponds to that of a liquid whose structure can continue to change with temperature. The low temperature branches of the LJ argon heat capacity and expansivity, by contrast, represent the properties of systems whose configurations have become fixed against further temperature decreases. The dashed line denoted MS in part (a) is from the fluid equation of state for LJ argon of I. R. McDonald and K. Singer, *Mol. Phys.* **23**, 29 (1972).

## DISPERSION CHARACTERISTICS AT VERY SHORT RELAXATION TIMES

In isothermal studies of dielectric relaxation, which can be carried out over very wide frequency ranges, it is commonly found for molecular liquids that the dispersion region cannot be characterized by a single relaxation time, i.e., the system returns to equilibrium after a perturbation in a nonexponential manner leading to a broader dispersion.<sup>24,25</sup> Frequently the width of the dispersion increases with decrease in temperature. Responses to mechanical perturbations (e.g., shear, longitudinal, isotropic compressional) cannot be evaluated as easily because of the more limited frequency ranges of the available techniques (e.g., three decades at most in ultrasonic studies, about a decade in Brillouin scattering) but, as best evaluated, are generally similar to the dielectric responses.<sup>25</sup>

For ionic liquids the electrical response is of different character, and tends to narrow in width with decreasing temperature.<sup>26</sup> In the few cases studied for which ultrasonic data are available,<sup>18,19</sup> the dispersion is qualitatively similar to that for molecular liquids, tending to be narrow at high temperatures and broader at low.

At gigahertz frequencies very little is known either for molecular or ionic liquids.

The recent Brillouin study of the  $\text{Ca}^{++}\text{--K}^{+}\text{--NO}_3^{-}$  system<sup>12</sup> suggested that in the short  $\tau$  region (i.e., at high temperatures) the dispersion is characterized by a single relaxation time, since single relaxation time theory gave, within measurement uncertainty, the temperature dependence measured for other transport properties in the same temperature range. Because the behavior of this simply constituted system is central to this paper we will examine its dispersion characteristics in more detail.

In relaxation studies employing a wide range of frequencies, it is common to present the real and imaginary parts of the complex susceptibility (e.g.,  $\epsilon'$  and  $\epsilon''$ ) or of the modulus ( $M'$  and  $M''$ ,  $M^* = 1/\epsilon^*$ ) both as isothermal functions of frequency for different temperatures and as a master plot combining results for different temperatures. In the master plot, the isothermal functions are collapsed on to a single curve (if the dispersion is temperature independent) by plotting  $M'$  and  $M''$  as a function of  $\omega\tau$  where  $\tau$  is either the average or the most probable relaxation time at each temperature. For the present  $\text{Ca}^{++}\text{--K}^{+}\text{--NO}_3^{-}$  case, only two frequencies per isotherm are available,<sup>12</sup> but these suffice. To construct this plot we need an average relaxation time for each temperature which should be chosen without any assumptions about the dispersion characteristics themselves (such as the single  $\tau$  assumption used in obtaining  $\tau_L$  in Ref. 12). We could either (i) assume the average longitudinal relaxation time to be the same as the average shear relaxation time, and plot  $M'$  and  $M''$  vs  $\omega\langle\tau_s\rangle$ , where  $\langle\tau_s\rangle$  is obtained from the relation

$$\langle\tau_s\rangle = \eta_s / G_\infty, \quad (2)$$

in which  $\eta_s$  is the shear viscosity and  $G_\infty$  is the infinite frequency shear modulus. ( $G_\infty$  is obtained from measurements on the velocity of shear waves observed near the glass transition, preferably using hypersonic frequencies<sup>19,20</sup> because of the greater range of dispersion-free data available.) Alternatively, we could (ii) follow the theory of Drake *et al.*<sup>27</sup> to obtain the average Mountain (longitudinal) relaxation time, as

$$\langle\tau_m\rangle = \eta_s \frac{M_\infty}{M_0(M_\infty - M_0)} \left( \frac{C_p^0 \eta_{v,s}}{C_p^\infty \eta_s} + \frac{4}{3} \right) \approx \eta_s \frac{10}{3} \frac{M_\infty}{M_0(M_\infty - M_0)} \quad (3)$$

(where the subscripts 0 and  $\infty$  refer to relaxed and frozen structures, respectively,  $C_p$  is the constant pressure heat capacity at the temperatures of interest, and  $\eta_{v,s}$  is the adiabatic bulk viscosity), and plot our  $M'$  and  $M''$  data vs  $\omega\langle\tau_m\rangle$  as in Ref. 27.

In each case the temperature dependence of  $\langle\tau\rangle$  is dominated by that of  $\eta_s$ , the influence of the temperature dependence of the modulus only being relative-

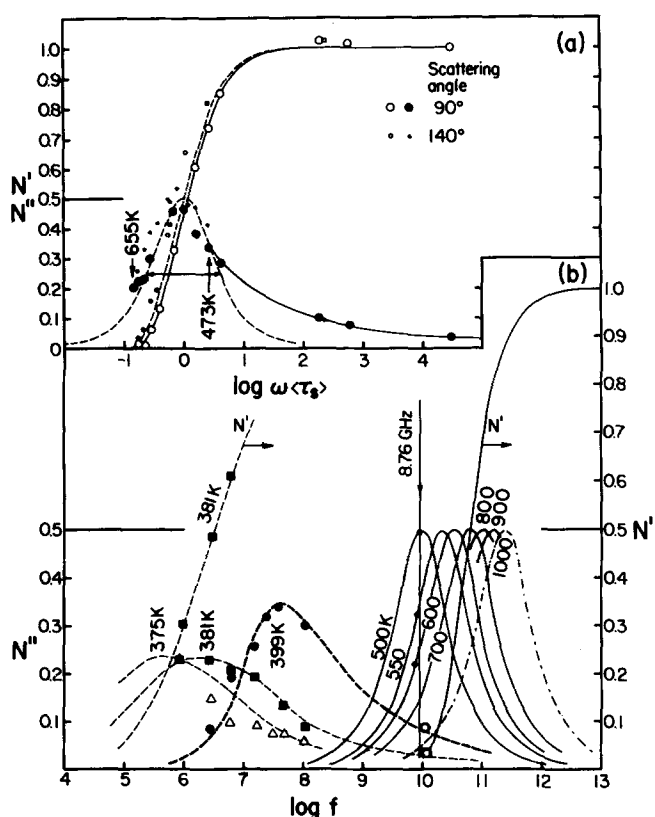


FIG. 4. Part (a)—Real and imaginary parts of the normalized longitudinal modulus  $N'$  and  $N''$  for the system  $\text{Ca}^{++}\text{-K}^+\text{NO}_3^-$ , obtained using hypersonic data from a range of temperatures and plotting against  $\omega \langle \tau_s \rangle$  where  $\tau_s$  is the average shear relaxation time. Dashed lines represent calculated single relaxation time curves. The Lorentzian (dashed line) form of the experimental data for  $N'$  and  $N''$  shows that a single relaxation time behavior exists in the temperature range 475–650 K. The solid line through the high  $\omega \langle \tau_s \rangle$  points for  $N''$  is only to emphasize the experimental behavior at low temperature. Part (b)—Real and imaginary parts of the normalized longitudinal modulus shown as a function of frequency for the nitrate melt at different temperatures, incorporating data from the ultrasonic study of Weiler *et al.* (Ref. 29). Note how the high temperature Lorentzian loss spectra (solid lines), based on the findings from part (a), develop into broad asymmetric loss spectra (dashed lines) at the lower temperatures. The heavy dashed line through the points at 399 K (filled and open circles for ultrasonic and Brillouin results, respectively) is a Cole-Davidson function with width parameter  $\alpha$  equal to 0.35. The frequency of the hypersonic phonon corresponding to the absorption maximum for light scattering 8.76 GHz is marked by a vertical arrow. Intersections with the  $N''$  isotherms give an approximate account of the temperature dependence of the absorption coefficient in the Brillouin scattering experiment [Ref. 12 and Fig. 2(a)].

ly significant at the highest temperatures. A calculation of  $\langle \tau_m \rangle$  using Eq. (3) yields a value which is about a factor of 2 longer than the value  $\tau_L$  obtained directly from the absorption maximum  $\omega \tau_L = 1$ , at the same temperature. Since  $\langle \tau_s \rangle$  has been shown<sup>12</sup> to agree with  $\tau_L$ , and since some of the parameters in Eq. (3) are not precisely known for the present system, it seems more appropriate to choose  $\langle \tau_s \rangle$ . Thus in Fig. 4(a) we plot, against  $\omega \langle \tau_s \rangle$ , the dimensionless normalized moduli  $N'$  and  $N''$  defined by

$$N' = \frac{M_\infty - M'}{M_\infty - M_0} = \frac{v_0^2 - v^2}{v_\infty^2 - v_0^2}, \quad (4)$$

$$N'' = \frac{M''}{M_\infty - M_0} = \frac{2\alpha v^3}{\omega(v_\infty^2 - v_0^2)} \quad (5)$$

Figure 4(a) is of considerable interest. Since a single relaxation time process is characterized by a loss spectrum  $M''$ , or  $N''$ , of Lorentzian shape (full width at half-height = 1.14 decades of frequency) and of height one half the full dispersion in  $N'$ , Fig. 5 shows that to good approximation (essentially within experimental uncertainty) the present relaxation process is indeed characterized by a single relaxation time for all temperatures above about 473 K. This means that the family of isothermal loss curves for temperatures above 473 K can be simply represented, as in Fig. 4(b), by a series of Lorentzians (solid lines) whose maxima occur at frequencies  $1/(2\pi\tau)$ .  $\tau$  is either calculated directly from the hypersonic data as in Ref. 12, or taken as  $\eta_s/G_\infty$  [Eq. (2)] using the precise  $\eta_s$  data available in this temperature range,<sup>18,19,28</sup> and the new  $G_\infty$  data now available from recent transverse phonon velocity measurements at hypersonic frequencies.<sup>20</sup> The latter source of  $\tau$  is preferable for  $\tau \gg \omega^{-1}$ .

The family of Lorentzians in Fig. 4(b) is helpful in appreciating how the absorption of a hypersonic wave will be affected by structural relaxation at the highest temperatures even at those above the decomposition point ~750 K for this system (dot-dashed lines). For instance, the vertical line in Fig. 4(b) represents a constant probe (excited phonon) frequency of about the average value of the Brillouin experiment, and it can be seen how it cuts even the 700 K isotherm at a significant value of the normalized mechanical loss  $N''$ . This is due essentially to the small displacement of the absorption curve along the frequency axis for a large change in temperature at high temperatures, a feature of the system's behavior which is at the heart of the smeared-out glass transition for fast experiments as we will detail in the next section.

Before leaving the present section, however, we must comment on the high  $\omega\tau$  behavior (low temperature absorption) in Fig. 4(a). Here it is clear that a major departure from the simplicity of the high temperature region has occurred, i.e., a single relaxation time theory is not valid for low temperatures.

The spread of the absorption over many decades in  $\omega\tau$  revealed by the low temperature points, means that the isothermal loss functions must have become very temperature dependent, as indeed the earlier ultrasonic work of Weiler *et al.*<sup>29</sup> had shown. Unfortunately, it is in this temperature region where the system tends to crystallize easily and, accordingly, few data could be obtained.<sup>12</sup> We can, however, combine the hypersonic with the ultrasonic data at 399 K to produce a reasonably complete isothermal loss spectrum in this complex region, and this is shown as a thick dashed line with data points in Fig. 4(b). This curve corresponds well to a Cole-Davidson distribution function with width parameter  $\beta = 0.35$  from which the dashed curve is calculated. This is the form and the width reported by Glover and

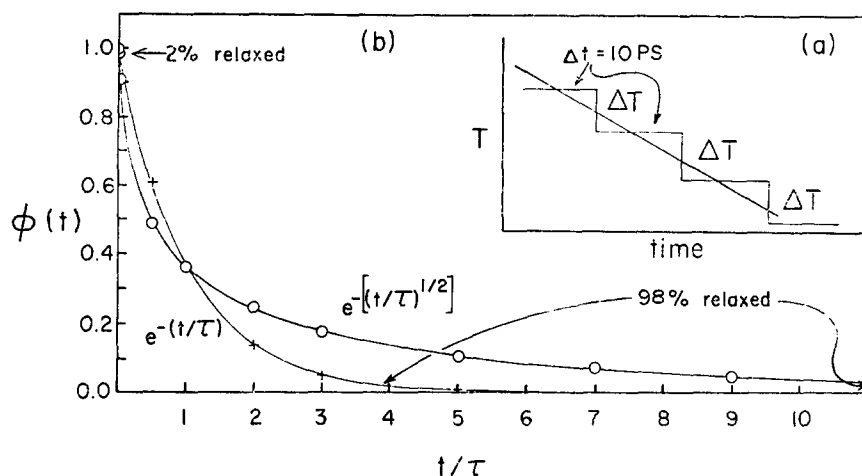


FIG. 5. (a) Representation of the temperature-time history of a computer simulation run and its equivalent cooling rate. Part (b) Representation of the relaxation to equilibrium following a perturbation at time 0 of a system property  $P$ , in units of the relaxation parameter  $\tau$ , for two relaxation functions, the simple exponential function and the fractional  $(1/2)$  exponential function. The figure illustrates the span in  $t/\tau$  over which perturbations from equilibrium pass from the just-detectably (2%) relaxed to the still-detectably unrelaxed (98%) condition. Similar spans in  $\tau/t$  apply to relaxation during stepwise (isochronal) cooling experiments.

Matheson for the shear modulus at low temperatures.<sup>19</sup> The shape of this loss spectrum could however, be reproduced almost as faithfully by a Fourier transform of the "fractional exponential" relaxation function

$$\phi(t) = \exp[-(t/\tau)^\beta] \quad (6)$$

long applied to the description of mechanical relaxations<sup>25</sup> and recently being widely adopted for use with dielectric and electrical relaxations.<sup>25,26,30,31</sup> For the 399 K isotherm the value of  $\beta$  would be 0.55, a value typical of relaxation in molecular liquids.<sup>25</sup> The 375 and 381 K (dashed) curves are reproductions of the Weiler *et al.* ultrasonic findings<sup>29</sup> at lower temperatures and represent an even broader distribution [ $\beta$  of Eq. (6) = 0.4] approaching that reported on the basis of enthalpy relaxation measurements at the glass transition.<sup>32</sup>

With the additional high frequency data it seems clear that the distribution of  $\tau$  for low temperatures is not simply Gaussian in  $\ln \tau$  as supposed in Ref. 29, but rather is remarkably extended to high frequencies for reasons not fully understood at this time. There is nothing in the heats of mixing for this system<sup>33</sup> to suggest any tendency to develop large composition fluctuations at low temperatures. It is quite possible that this is the normal behavior pattern for simply constituted systems, rather few of which have been characterized over the frequency range and temperature range of the present system. Dispersions of the form of the 399 K isotherm are, however, very common for molecular liquids in the vicinity of  $T_g$ . Broader relaxations like those at 375 and 381 K are known for certain polymers.<sup>31</sup>

Figure 4(b) now gives a fairly comprehensive picture of the relaxation characteristics of the present system, and permits us to interpret the fast phenomena of Fig. 3 in a satisfactory general manner, as follows.

### THE TEMPERATURE DEPENDENCE OF THE RELAXATION TIME AND THE FAST GLASS TRANSITION

To appreciate how the isothermal relaxation function [Eq. (6)] and the temperature dependence of the relaxation time combine to determine the form of the glass transition, (or the dispersion in temperature for a fixed

frequency probe) it is helpful to consider cooling as a succession of equal temperature downsteps, the time between which is determined by the cooling rate [Fig. 5(a)]. Each step is considered small enough that the response to the perturbation of the equilibrium state is essentially linear. The approach to equilibrium can, in the simplest case where  $\tau$  is single valued, be depicted by an exponential function of time where  $\tau$ , the relaxation time, is determined by the time taken for the perturbation, to fall to  $1/e$ th of its initial value [Fig. 5(b)].

In units of  $\tau$ ,  $t$  must vary by a factor of about 100 for the extent of relaxation to pass from very little ( $\sim 2\%$  at  $0.05 \tau$ ) to almost complete ( $\sim 98\%$  at  $5\tau$ ). For a given cooling rate [fixed value of  $\Delta t$  in Fig. 5(a)], the system will remain in equilibrium so long as  $\Delta t$  is long with respect to  $5\tau$  where  $\tau$  now varies with temperature, increasing with decreasing  $T$ . When  $\Delta t \sim 5\tau$ , equilibration will only be 98% complete before another  $\Delta T$  occurs.  $\tau$  then becomes still longer and approach to equilibrium consequently becomes still more sluggish and incomplete. From there on, the system rapidly falls out of equilibrium and vitrifies. The temperature range over which equilibrium will be lost and dispersion observed, will be that needed to change the relaxation time by some two orders of magnitude if the relaxation is single. Alternatively, it will be that needed to change the *average* relaxation time by 3–4 orders of magnitude if the relaxation has a broad distribution in  $\tau$ , e.g.,  $\exp\{-[t/\tau]^{1/2}\}$ , Fig. 5.

The dispersion range in temperature must thus depend heavily on how rapidly  $\tau$  changes with  $\Delta T$ , i.e., on the "activation energy"  $E_a$  for  $\tau$ . These may be seen from the Arrhenius plot (Fig. 6), in which shear relaxation  $\langle \tau_s \rangle$  data based on Eq. (5), longitudinal relaxation  $\tau_L$  data from direct observations,<sup>12</sup> and conductivity relaxation  $\langle \tau_\sigma \rangle$  data,<sup>26</sup> are all collected together. A single, rather approximate value for the  $\text{NO}_3$  reorientation time, derived<sup>34</sup> from a combination of polarized and depolarized Raman scattering measurements by Clarke and Miller,<sup>35</sup> is included for comparison.

Figure 6 shows that at high temperatures 475–675 K,  $\tau$  varies slowly with temperature, i.e.,  $E_a$  is small,



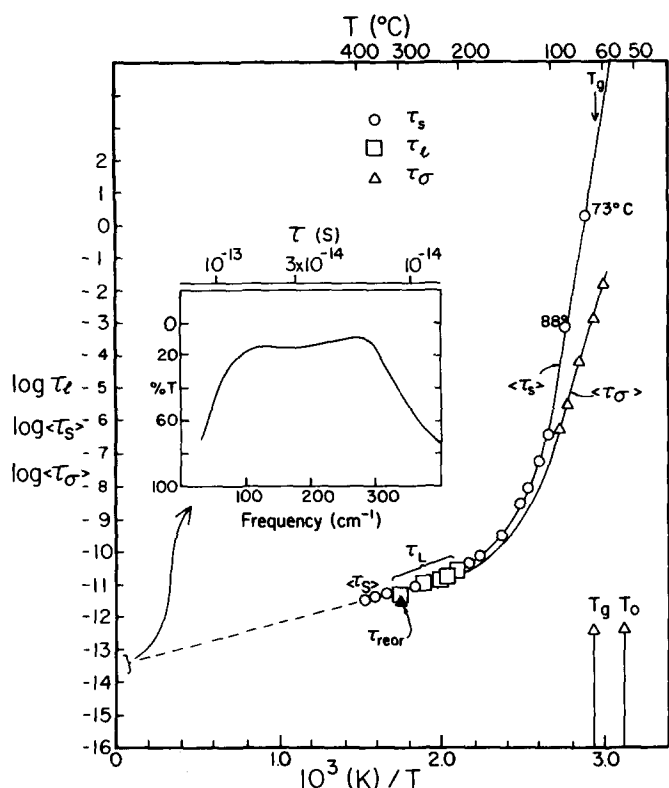


FIG. 6. Arrhenius plot of the longitudinal relaxation time from the Brillouin scattering experiments  $\tau_L$ , the average shear relaxation time  $\langle\tau_s\rangle$  obtained from Eq. (2), and the average conductivity relaxation times  $\langle\tau_\sigma\rangle$  taken from Ref. 26. A value for the nitrate ion reorientation time obtained from Raman linewidth data by Clarke and Miller (Ref. 35) is also included (solid triangle). Insert: Far infrared absorption band showing the coupled transverse vibrational modes of the quasilattice (Ref. 39). It is this band of frequencies to which the relaxation times plotted in the main diagram extrapolate at  $1/T=0$ .

and a large interval of temperature  $> 200$  K is needed to change  $\tau$  by two orders of magnitude. Thus any measurement whose time scale is short enough to give a dispersion maximum  $\omega\tau = 1$  in this temperature range will inevitably show a very broad dispersion range in temperature, even if the process under study is characterized by a single relaxation time. By contrast, if the measurement is a slow one so that the dispersion maximum occurs in the low temperature region where the temperature coefficient of  $\tau$  is very large, then even in the presence of a broad distribution of  $\tau$  [highly nonexponential relaxation, or  $\beta$  of Eq. (6)  $\ll 1$ ], the dispersion will be quite narrow because  $\langle\tau\rangle$  changes by four orders of magnitude in a temperature interval of a mere  $15^\circ$  near  $T_g$ , see Fig. 6.

A small activation energy for relaxation in the *high fluidity* regime is characteristic of liquids in general. We give some examples below, but note first that for comparisons amongst different liquids in this region, the activation energies should be reduced by the temperature  $T_{ref}$  at some standard short relaxation time, e.g.,  $2 \times 10^{-11}$  s. Thus for  $\text{Ca}^{++}\text{-K}^+\text{-NO}_3^{12}$   $E_a/RT_{ref} = 37600/8.03 \times 493 = 9.50$ , for LJ argon<sup>4</sup>  $E_a/RT_{ref} = 3763/8.03 \times 45 = 10.4$ , for water  $E_a/RT_{ref}^{36} = 18800/8.03 \times 273 = 8.2$ , and for *o*-terphenyl<sup>37</sup>  $E_a/RT_{ref} = 30000/$

$8.03 \times 370 = 10.1$ . Therefore all liquids (excepting perhaps some strong network cases where  $E_a$  remains large at high fluidities) should show a very broad temperature dispersion in hypersonic experiments, and a very extended glass transformation range in ultra-fast quenching processes.

It is important to recognize that over the  $\sim 200$  K temperature interval (600–400 K) in which loss of equilibrium in liquid  $\text{Ca}^{++}\text{-K}^+\text{-NO}_3$  would occur progressively during hyperquenching (on the simulation time scale) (see Fig. 3), the density of the  $\text{Ca}^{++}\text{-K}^+\text{-NO}_3$  melt changes from 1.913 to 2.189 g cc<sup>-1</sup>. This is about 70% of the total density change observable in the liquid range between  $T_g$  and 750 K at which decomposition occurs. Thus the notion of a "fictive" temperature in its normal sense of a "structural" temperature at which the glass structure is that of the equilibrium fluid is a much less satisfactory concept for hyperquenched than for normal and, particularly, annealed glasses. The fictive temperature concept would only be useful if, as is often assumed, increase of cooling rate or frequency simply shifted the sharp low temperature dispersion in Fig. 2(c) along the  $T$  axis. It is not clear how the relation between the glass and liquid structures should be described in hyperquenched cases.

This dilemma, as we have shown, results from the difference in temperature dependence of  $\tau$  in the high and low temperature regimes. In the next section we examine in general terms the origin of this temperature dependence, using the short relaxation time data to make some useful new correlations.

## THE GENERAL FORM OF $\tau$ VS $T$

Our understanding of fast glass transition problems will be much improved if we can tie  $\text{Ca}^{++}\text{-K}^+\text{-NO}_3$  and LJ argon into a common pattern with respect to high and low temperature limiting relaxation characteristics. Again, we commence with the experimental case, and extend the ideas to the simulation results.

Figure 6 is very helpful with respect to establishing the lower (i.e., high temperature) limit on  $\tau$ . Thanks to the support given the viscosity-based  $\langle\tau_s\rangle$  values by the direct  $\tau_L$  determinations (which are themselves only of good accuracy near  $\omega\tau = 1$ ), a natural extrapolation to  $1/T = 0$  can be made. This yields a rather significant result. The extrapolation carries  $\tau$  directly into the region of the inverse quasilattice frequencies determined by far IR spectroscopy.<sup>38</sup> The far IR spectrum for a thin (30  $\mu$ ) film of  $\text{Ca}^{++}\text{-K}^+\text{-NO}_3$  (Ca:K = 2:3) glass<sup>39</sup> is reproduced in the inset to Fig. 6 using both wave number and cycle time scales. Thus the lower limit on  $\tau$ , in accord with the interpretation qualitatively associated with Arrhenius equation preexponents, but rarely directly demonstrated as in Fig. 6, is some average over the time required for the components of the liquid quasilattice to move relative to one another (the necessary preliminary to disengagement and rearrangement). The corresponding quasilattice frequency for LJ argon is centered at  $\sim 65$  cm<sup>-1</sup>, according to Rahman *et al.*<sup>40</sup>

At the low temperature end  $\tau$  is unbounded, except



for quantum fluids, and the question to be answered is how is the very long  $\tau$  regime ( $\tau$  of order hours, and longer than most experiments) approached as the temperature decreases, particularly in the vicinity of the glass transition temperature.

Figure 6 shows that for the case of  $\text{Ca}^{++}\text{-K}^+\text{-NO}_3^-$ , the Arrhenius coefficient (apparent activation energy) undergoes an enormous increase as temperature decreases. The greatest part of this change occurs where the loss spectrum,  $N''$  in Fig. 4, broadens out. In this region ( $T = 400\text{--}500\text{ K}$ )  $\tau$ , and the common transport properties, viscosity, conductivity, and several ionic diffusivities, as well, all seem to be well described<sup>41</sup> by the Vogel–Tammann–Fulcher VTF equation which contains a parameter representing a temperature  $T_0 = 321\text{ K}$  (the so-called ideal glass transition temperature) at which  $\tau$  would go to infinity:

$$\tau = A_r \exp B/(T - T_0) . \quad (7)$$

If we assume argon is phenomenologically similar to  $\text{Ca}^{++}\text{-K}^+\text{-NO}_3^-$  we may estimate a value of  $T_0$  for argon by scaling the nitrate value  $T_0 = 321\text{ K}$  down to the argon temperature range using the ratio of the two dispersion midpoint temperatures. This yields a temperature  $T_0$  for argon of  $321\text{ K} \times 38/493 \sim 25\text{ K}$ , if we use the  $C_p$  results of Clarke,<sup>7</sup> and  $\sim 27\text{ K}$  if we use the corresponding expansivity data, see Fig. 3. (The Fox–Andersen midpoint temperature is lower by 12 K in the direction expected from their much slower cooling rate and truncated LJ potential.) Interestingly enough, the above  $T_0$  values are in the range 24–27 K of the Kauzmann temperature  $T_K$ , at which a comparison of argon liquid and crystal state entropies in the supercooled region (but above the transformation region) shows<sup>7,10</sup> the excess entropy of liquid over crystal would vanish. The coincidence of  $T_0$  of Eq. (7) with the temperature of vanishing excess entropy  $T_K$  has been discussed in detail elsewhere,<sup>25,42–46</sup> and suggests that the factor responsible for the great increase in activation energy and relaxation time at low temperatures is the rapid decrease in availability of configurational microstates as  $T$  approaches  $T_0$ .<sup>42</sup> Thus it would seem that  $\tau$  is constrained by thermodynamic considerations to become very long at a temperature which is far above 0 K, and which can be estimated from calorimetric data.

It is evidently this latter circumstance which directly forces the change from low to high activation energy with increasing relaxation time, hence is responsible for the sharpening up of the glass transition.

## THE CRYSTALLIZATION CURTAIN

Examined in the short time regime, the behavior of the simplest fluids and of their nearest glass-forming equivalents, seem from all the above to be impressively similar. Furthermore, in the most recent hard sphere<sup>47,48</sup> and LJ<sup>8</sup> studies, non-Arrhenius transport behavior has been observed to conform to relations of the form of Eq. (7) for both temperature and volume dependence. One study on LJ argon has even briefly addressed the problem of the stress relaxation function

in the glassy state,<sup>49</sup> and shown it to be far from exponential (though the conditions of the simulation—temperature and density—unfortunately were not specified). The wide time scale range of the Fox–Andersen study on the LJ system<sup>8</sup> suggests that the interesting temperature regime in which single  $\tau$  behavior is lost (see Fig. 4) should be investigable by computer simulation.

The outstanding difference between the simple LJ and the “quite simple”  $\text{Ca}^{++}\text{-K}^+\text{-NO}_3^-$  systems, then, seems to lie in the time scale on which the former escapes from the metastable state. It is beyond the scope of the present paper to enter this important question in any depth, but it is desirable to place it in time scale perspective to the relaxation processes we have been considering here. The difference in “escape time” arises primarily because of the fact that simple atomic fluids have “high” melting points, i. e., they become metastable with respect to their crystal phases at temperatures where the time scale for exploration of the fluid phase space is very short (see Fig. 1 of Ref. 4). The result is that the relatively rare fluctuations which create “escape channels” between fluid and crystal phase space via the creation of “critical nuclei” are accessed on time scales of nanoseconds during cooling,<sup>40</sup> and even less if fast cooling through the critical (maximum nucleation rate) region to low temperatures is followed by reheating.<sup>8</sup>

The latter circumstance implies that, in the absence of nuclei-destroying Maxwell demons, it is impossible to answer the question of how LJ argon would behave at the “ordinary” glass transition ( $\tau = 20\text{--}200\text{ s}$ ) because the internally equilibrated structure which would have this characteristic relaxation time cannot be produced in principle, i. e., even in computer simulations for which unlimited machine time is available. It is for the same reason that glass transitions (hence internally equilibrated states) cannot be observed at ordinary heating rates in the majority of splat-quenched amorphous alloys. These are all near the edge of the “doubly unstable” region<sup>50</sup> where any attempt to restore amorphous phase equilibrium produces a structure which relaxes more rapidly out of amorphous phase space than within it, implying that a *mechanically unstable state* is encountered.

It will be interesting to see to what extent the study of relaxation phenomena by simulation can be extended by using mixtures of LJ particles to stabilize the liquid phase,<sup>51</sup> or subtle pair potentials, e. g., with icosahedral direction-dependent components<sup>52</sup> which destabilize the ordered state.<sup>52</sup>

## ACKNOWLEDGMENTS

We are indebted to the U. S. National Science Foundation (under Solid State Chemistry Grant No. DMR 7302632A01) and the Swedish Natural Research Council for support of this work. We thank C. J. Montrose for discussion of current theory and M. Goldstein for some helpful comments on the manuscript.

- <sup>1</sup>G. O. Jones, *Glass* (Methuen, London, 1954).
- <sup>2</sup>H. S. Chen and D. Turnbull, *Appl. Phys. Lett.* **10**, 284 (1967).
- <sup>3</sup>D. E. Polk and W. C. Giessen in *Metallic Glasses*, edited by J. J. Gilman and H. J. Leamy (American Society for Metals, Metals Park, Ohio, 1978), Chap. 1.
- <sup>4</sup>C.-J. Lin and F. Spaepen, *Appl. Phys. Lett.* **41**, 721 (1982).
- <sup>5</sup>C. S. Hsu and A. Rahman, *J. Chem. Phys.* **70**, 5234 (1979); **71**, 4974 (1979).
- <sup>6</sup>W. Damgaard Kristensen, *J. Non-Cryst. Solids* **21**, 303 (1976).
- <sup>7</sup>J. H. R. Clarke, *J. Chem. Soc. Faraday Trans. 2*, 1371 (1979).
- <sup>8</sup>G. Fox and H. C. Andersen, *Ann. N. Y. Acad. Sci.* **371**, 123 (1981); H. C. Andersen (private communication).
- <sup>9</sup>F. F. Abraham, *J. Chem. Phys.* **72**, 359 (1980).
- <sup>10</sup>L. V. Woodcock, C. A. Angell, and P. Cheeseman, *J. Chem. Phys.* **65**, 1565 (1976); C. A. Angell, J. H. R. Clarke, and L. V. Woodcock, *Adv. Chem. Phys.* **48**, 397 (1981).
- <sup>11</sup>C. A. Angell, *Ann. N. Y. Acad. Sci.* **371**, 136 (1981); (a) S. A. Rice, *Trans. Faraday Soc.* **58**, 499 (1962).
- <sup>12</sup>L. M. Torell, *J. Chem. Phys.* **76**, 3467 (1982).
- <sup>13</sup>C. T. Moynihan, H. Sasabe, and J. C. Tucker, in *Molten Salts*, Proceedings of the International Conference of Molten Salts, edited by J. P. Pemsler, J. Bronstein, D. R. Morris, K. Nobe, and N. E. Richards (The Electrochemical Soc., 1976), p. 182.
- <sup>14</sup>A. Barkatt and C. A. Angell, *J. Chem. Phys.* **70**, 901 (1979).
- <sup>15</sup>(a) P. F. Sullivan and G. Seidel, *Phys. Rev.* **173**, 679 (1968); (b) P. Handler, D. E. Mapother, and M. Raye, *Phys. Rev. Lett.* **19**, 356 (1967).
- <sup>16</sup>C. T. Moynihan, P. B. Macedo, C. J. Montrose, P. K. Gupta, M. A. DeBolt, J. F. Dill, B. E. Dom, P. W. Drake, A. J. Easteal, P. B. Elterman, R. P. Moeller, H. Sasabe, and J. A. Wilder, *Ann. N. Y. Acad. Sci.* **279**, 15 (1976).
- <sup>17</sup>L. M. Torell, *J. Acoust. Soc. Am.* **57**, 876 (1975).
- <sup>18</sup>H. Tweer, N. Laberge, and P. B. Macedo, *J. Am. Ceram. Soc.* **54**, 121 (1971).
- <sup>19</sup>G. M. Glover and A. J. Matheson, *Trans. Faraday Soc.* **67**, 1960 (1971).
- <sup>20</sup>L. M. Torell and R. Aronsson, *J. Chem. Phys.* (to be published).
- <sup>21</sup>K. Hertzfeld and T. A. Litovitz, *Absorption and Dispersion of Ultrasonic Waves* (Academic, New York, 1959), p. 475. The relation quoted is approximate, with connection terms of order  $\alpha v_L/w$ . For the present system this term is always small (0.1 or less) as can be seen from the well-defined Brillouin peaks even at maximum damping, see Ref. 12.
- <sup>22</sup>K. J. Rao, C. A. Angell, and D. B. Helphrey, *Phys. Chem. Glasses* **14**, 26 (1973).
- <sup>23</sup>C. T. Moynihan, A. J. Easteal, and J. C. Tucker, *J. Phys. Chem.* **78**, 26783 (1974).
- <sup>24</sup>G. Williams and P. J. Hains, *Faraday Symp. Chem. Soc.* **6**, 14 (1972).
- <sup>25</sup>Reviewed in J. Wong and C. A. Angell, *Glass: Structure by Spectroscopy* (Dekker, New York, 1976), Chap. 11.
- <sup>26</sup>F. S. Howell, R. A. Bose, P. B. Macedo, and C. T. Moynihan, *J. Phys. Chem.* **78**, 639 (1974).
- <sup>27</sup>P. W. Drake, J. F. Dill, C. J. Montrose, and R. Meister, *J. Chem. Phys.* **67**, 1969 (1977).
- <sup>28</sup>E. Rhodes, W. E. Smith, and A. R. Ubbelohde, *Trans. Faraday Soc.* **63**, 1943 (1967).
- <sup>29</sup>R. Weiler, R. Bose, and P. B. Macedo, *J. Chem. Phys.* **53**, 1258 (1970).
- <sup>30</sup>G. Williams and D. C. Watts, *Trans. Faraday Soc.* **66**, 80 (1970).
- <sup>31</sup>K. Ngai, *Solid State Ionics* **5**, 27 (1981).
- <sup>32</sup>C. T. Moynihan, H. Sasabe, and J. C. Tucker, in *Molten Salts*, edited by J. P. Pemsler, J. Bronstein, D. R. Morris, K. Nobe, and N. E. Richards (Electrochemical Society, 1976), p. 185.
- <sup>33</sup>O. J. Kleppa and L. S. Hersh, *Discuss. Faraday Soc.* **32**, 99 (1962).
- <sup>34</sup>C. A. Angell, in *Vibrational Spectroscopy in Molecular Liquids and Solids*, edited by E. M. Pick and S. Bratos (Plenum, New York, 1980), p. 187.
- <sup>35</sup>J. H. R. Clarke and S. Miller, *Chem. Phys. Lett.* **13**, 97 (1972).
- <sup>36</sup>W. M. Slie, A. R. Donfor, and T. A. Litovitz, *J. Chem. Phys.* **44**, 3712 (1966).
- <sup>37</sup>Y. Higashigaki and C. H. Wang, *J. Chem. Phys.* **74**, 3175 (1981). These authors' observations are closely related to those reported for the nitrate melt in Ref. 12 though their absorption maximum is not as well resolved. We believe the "kinks" they describe at a temperature designated  $T_k$  are best regarded as dispersion maxima in the sense of Figs. 2(a) and 4.
- <sup>38</sup>C. A. Angell and J. Wong, *J. Chem. Phys.* **51**, 4519 (1969).
- <sup>39</sup>J. Wong, Ph.D. thesis, Purdue University, 1970.
- <sup>40</sup>A. Rahman, M. J. Mandell, and J. P. McTague, *J. Chem. Phys.* **64**, 1564 (1976); A. Rahman, *J. Chem. Phys.* **136**, A405 (1964).
- <sup>41</sup>C. A. Angell and C. T. Moynihan, in *Molten Salts: Characterization and Analysis*, edited by G. Mamantov (Dekker, New York, 1969), p. 315.
- <sup>42</sup>G. Adam and J. H. Gibbs, *J. Chem. Phys.* **43**, 139 (1965).
- <sup>43</sup>M. Goldstein, *J. Chem. Phys.* **51**, 3728 (1969).
- <sup>44</sup>C. A. Angell and K. J. Rao, *J. Chem. Phys.* **57**, 470 (1972).
- <sup>45</sup>C. A. Angell and D. L. Smith, *J. Phys. Chem.* **86**, 3845 (1982).
- <sup>46</sup>C. A. Angell and W. J. Sichina, *Ann. N. Y. Acad. Sci.* **279**, 53 (1976).
- <sup>47</sup>L. V. Woodcock and C. A. Angell, *Phys. Rev. Lett.* **47**, 1129 (1981).
- <sup>48</sup>L. V. Woodcock, *Ann. N. Y. Acad. Sci.* **371**, 274 (1981).
- <sup>49</sup>M. Rekhson, D. M. Heyes, C. J. Montrose, and T. A. Litovitz, *J. Non-Cryst. Solids* **38**, **39**, 403 (1980).
- <sup>50</sup>C. A. Angell, E. J. Sare, J. Donella, and D. R. MacFarlane, *J. Phys. Chem.* **51**, 1461 (1981).
- <sup>51</sup>B. J. Alder, *J. Chem. Phys.* **40**, 2724 (1964).
- <sup>52</sup>P. J. Steinhardt, D. R. Nelson, and M. Ronchetti, *Phys. Rev. Lett.* **47**, 1297 (1981).